The Journal of Immunology

Clustering Class I MHC Modulates Sensitivity of T Cell Recognition

David R. Fooksman, Gigi Kwik Grönvall, Qing Tang and Michael Edidin

J Immunol 2006; 176:6673-6680; ;
doi: 10.4049/jimmunol.176.11.6673
http://www.jimmunol.org/content/176/11/6673

The Journal of Immunology is published twice each month by
The American Association of Immunologists, Inc.,
1451 Rockville Pike, Suite 650, Rockville, MD 20852

Print ISSN: 0022-1767 Online ISSN: 1550-6606.

Clustering Class I MHC Modulates Sensitivity of T Cell Recognition[1]

David R. Fooksman, Gigi Kwik Grönvall,[2] Qing Tang,[3] and Michael Edidin[4]

T cell recognition of peptide-MHC is highly specific and is sensitive to very low levels of agonist peptide; however, it is unclear how this effect is achieved or regulated. In this study we show that clustering class I MHC molecules on the cell surface of B lymphoblasts enhances their recognition by mouse and human T cells. We increased clustering of MHC I molecules by two methods, cholesterol depletion and direct cross-linking of a dimerizable MHC construct. Imaging showed that both treatments increased the size and intensity of MHC clusters on the cell surface. Enlarged clusters correlated with enhanced lysis and T cell effector function. Enhancements were peptide-specific and greatest at low concentrations of peptide. Clustering MHC class I enhanced recognition of both strong and weak agonists but not null peptide. Our results indicate that the lateral organization of MHC class I on the cell surface can modulate the sensitivity of T cell recognition of agonist peptide. *The Journal of Immunology,* **2006, 176: 6673–6680.**

The recognition of peptide-MHC molecules by $CD8^+$ cytotoxic T cells is a fundamental problem for immune function. T lymphocytes must constantly monitor APCs of the body to identify epitopes that indicate infection by pathogen or damaged tissue. However, to identify their targets, T cells must find a specific peptide-MHC molecule in a sea of noncognate self-peptide-MHC on a cell surface. These cognate peptides may be scarce and may also be weakly activating. It is particularly unclear how weak agonists are distinguished from self-peptide-MHC because their affinity for the TCR may, in some cases, be lower than that of nonactivating, antagonist peptides (1).

It has been shown that effector T cells can respond to cells displaying as little as 1–10 agonist-loaded MHC on the surface (2–5). These studies have focused on strongly activating agonist peptides with high affinities for both MHC class I and TCR. However, the molecular stoichiometry for binding strong agonists may not hold for weaker agonists. Furthermore, higher concentrations of agonist certainly engender better responses, and surface MHC loaded with noncognate peptides may also contribute to recognition (5). We still lack a comprehensive model to explain the full nature of T cell recognition of cognate peptide-MHC.

Part of the answer to the problem of a T cell maintaining high specificity and sensitivity to low levels of Ag may lie in the organization of MHC molecules on the surface of an APC. Biophysical studies have shown that class I MHC molecules are not randomly distributed on the surface of APCs and that disrupting their organization affects recognition of MHC molecules by CTLs. Native class I MHC molecules cluster in the presence of free class I MHC H chains (6). Integrins, class II MHC molecules, and the IL-2R are also found in association with class I MHC on the cell surface (7). When these clusters are dissipated with exogenous β_2-microglobulin, Ag presentation is reduced (8). These studies indicate that the surface organization of class I MHC molecules contributes to their function and suggest that surface MHC organization may participate in T cell recognition of agonist peptide. Because clusters of class I MHC molecules contain both agonist and noncognate endogenous peptides, these mixed-peptide bouquets may enhance recognition of agonist peptides complexes contained within them.

Surface organization of class I MHC molecules can be modulated by addition or removal of cholesterol to and from the cell membrane (9); this results in changes in clustering detected by FRET (fluorescence resonance energy transfer) and in reductions in lateral mobility and diffusibility (10). The mechanism of immobilization after cholesterol depletion appears to involve release of the signaling lipid phosphatidylinositol 4,5-bis-phosphate from the membrane inner leaflet and a consequent reorganization of cell actin (10). Stabilizing the actin membrane skeleton corrals membrane proteins and enhances their clustering on the cell surface (11, 12). In this study, we show that these cholesterol-depleted cells present peptide-MHC Ag better than control cells and that this enhanced presentation correlates with changes in class I MHC cluster size. Enhanced presentation is peptide-specific and is most effective at low levels of agonist peptide-MHC. We further show that clustering of class I MHC by another mechanism, direct cross-linking of engineered class I MHC molecules, also enhances presentation of peptide-MHC to T cells, again enhancement is greatest when agonist peptide is scarce. Our results suggest that clustering enhances TCR scanning for and recognition of agonist peptide.

Materials and Methods

Cell lines and treatments

Cells were maintained in RPMI 1640 (Mediatech) plus 2 mM glutamine, 10% heat-inactivated FBS (HyClone Laboratories), and 300 μg/ml G418 (Sigma-Aldrich) for plasmid selection, when applicable. JY B lymphoblasts were a gift from J. Strominger, Harvard University (Cambridge, MA). T2 (13), T2-K^b (14), and 2C T cells (15), both naive and activated, were provided by J. Schneck, Department of Pathology, Johns Hopkins Medical Institutions (JHMI, Baltimore, MD).

Department of Biology, Johns Hopkins University, Baltimore, MD 21218

Received for publication October 12, 2005. Accepted for publication March 13, 2006.

The costs of publication of this article were defrayed in part by the payment of page charges. This article must therefore be hereby marked *advertisement* in accordance with 18 U.S.C. Section 1734 solely to indicate this fact.

[1] This work was supported by an award from the Center for Alternatives to Animal Testing, Johns Hopkins University (to G.K.G.), and by National Institutes of Health Research Grants AI-14584 and GM058554 (to M.E.) and Training Grant T32 GM07231 to the Department of Biology, Johns Hopkins University.

[2] Current address: Center for Biosecurity, University of Pittsburgh Medical Center, 621 East Pratt Street, Suite 210, Baltimore, MD 21202.

[3] Current address: Leica Microsystems, 2345 Waukegan Road, Bannockburn, IL 60015.

[4] Address correspondence and reprint requests to Dr. Michael Edidin, Department of Biology, Johns Hopkins University, 3400 North Charles Street, Baltimore, MD 21218. E-mail address: edidin@jhu.edu

0022-1767/06/$02.00

Activated 2C T cells were generated in the Schneck laboratory by isolating splenocytes, activating with 1 μg/ml agonist SIY peptide for 4 days, and then culturing with 10 U/ml IL-2 (Sigma-Aldrich) for an additional 3–6 days. Naive CD8$^+$ T cells were purified by negative selection by MACS. Allogenic A2-negative T cells were provided by the Laboratory of Immunogenetics (JHMI). Cells from one donor, the senior author, were used for all experiments. Allo-T cells were activated by coculture with irradiated JY (A2-positive) cells for 4 days.

JY target cells were acutely depleted of cholesterol by 1 h incubation with 0.5 U/ml cholesterol oxidase (no. C5421; Sigma-Aldrich) or 10 mM methyl-β-cyclodextrin (Sigma-Aldrich) for 30 min for total internal reflection fluorescence microscopy (TIRFM)[5] imaging. Chronic depletion was achieved by culturing cells in medium with 10% FBS lacking low-density lipoprotein (LDL; InvivoGen) for 3–14 days. Cell levels of cholesterol were reduced to 50–60% of control by this chronic deprivation. As we noted earlier (10), the effect of cholesterol depletion on lateral mobility was not reversed by growing cells in LDL-containing medium for 12 h, though it was reversed after 24–36 h. Actin cytoskeleton was disrupted in JY cells by incubating them with 5 μg/ml cytochalasin D (CytD; Sigma-Aldrich) for 30 min at 37°C, followed by extensive washing.

T2 cell lines were incubated overnight at 25°C, and then pulsed with peptide in serum-containing medium for 1–2 h at 37°C. The peptides used were SIY (SIYRYYGL), SIN, (SIINFEKL), and p2CA (LSPFPFDL) (1). After peptide loading, cells were treated for 2 h with 10 nM AP20187 dimerizer from the Ariad Regulated Homodimerization kit (⟨www.ariad.com⟩) and washed, extensively. When T2 Kb-1BP cells were used to stimulate naive CD8$^+$ 2C T cells, they were incubated with 0.01 nM dimerizer for the duration of the stimulation.

Construction of cross-link H2-K^b, Kb-1BP

Kb-1BP was cloned into the N3-YFP vector (BD Clontech) using PCR linkers. Mouse class I H2-K^b H chain was tagged with a C-terminal yellow fluorescent protein (YFP), as described previously (16). A single FKBP domain was excised from the pC4-Fv1E plasmid (Ariad Pharmaceuticals) and inserted, in-frame and downstream of YFP using *Xba*I and *Bam*HI sites in both plasmids. Monomeric YFP mutation L221K (17) was added by QuikChange (Stratagene), and the entire open reading frame was sequenced in both orientations to confirm no additional point mutations had been introduced. The HLA-A2-YFP used for JY TIRFM imaging was described earlier (18).

Cells were transfected by electroporation using 10–20 μg of plasmid DNA. For JY A2-YFP cells, these cells were selected for expression using 300 μg/ml G418, followed by FACS sorting for high expressors. We were unable to create stable clones of T2-expressing Kb-1BP at moderate to high levels. Hence, for all experiments with the construct, T2 were transfected with Kb-1BP and used for assays 24–36 h later.

Microscopy

T2 Kb-1BP cells were fixed in 4% paraformaldehyde (catalog no. 15710; Electron Microscopy Sciences) for 30 min on ice. Cells were washed and then plated on poly-L-lysine-coated (Sigma-Aldrich) coverslips for 5 min, and then mounted with SlowFade Gold (Invitrogen Life Technologies). Confocal microscope z-stack images were taken on a Zeiss LSM510 Meta with a ×63 objective with appropriate YFP filters, PMT detector and resolution settings. Settings were kept constant for all images.

For TIRFM, live A2-YFP JY cells were plated on poly-L-lysine-coated sapphire coverslips and maintained at 37°C by a Focht Chamber System 2 live cell chamber (Bioptechs). Images were taken on an Olympus IX-70 microscope using ×100 1.65NA objective and a Cooke SensiCamQE CCD camera. Detection settings were kept constant between treatments.

Clusters were captured from images using NIH Image (or ImageJ) software above a constant threshold and then analyzed using Origin 7.0 (MicroCal), GraphPad 4.0 (Prism), and Excel (Microsoft) to generate distributions for cluster size and intensity. For images of Kb-1BP with or without dimerizer, distributions of cluster mean intensity was compared by using a (Gaussian) Student *t* test in GraphPad 4.0. Cluster size distributions for treated and untreated were compared by nonparametric *t* test assuming equal variances.

T cell functional assays

For chromium release assays, target cells were incubated with 100 μCi ^{51}Cr (PerkinElmer) for 1 h at 37°C, washed three times, and incubated with effector cells at ranges from 10:1 to 1:4 E:T ratio, keeping the target cell number fixed at 1×10^4 cells and the volume of medium at 200 μl in 96-well round-bottom plates. After 4 h, cells were centrifuged, and 100 μl of supernatant was measured for ^{51}Cr using a Beckman 5500 gamma counter. Experiments were conducted in triplicate and compared with spontaneous release of targets alone and maximal release of targets in 1 M HCl. Specific lysis was calculated as 100 × (experimental − spontaneous)/(maximal − spontaneous).

Serine esterase release was measured with T cells mixed at a 10:1 ratio with JY cells for 4 h. Supernatants were harvested and serine esterases were detected in a colorimetric assay as described previously (19). To provoke maximal release, effectors were treated with 40 ng/ml PMA (catalog no. 13139019; Sigma-Aldrich) and 2 μg/ml calcium ionophore (catalog no. 7522; Sigma-Aldrich). Percentage release was calculated as 100 × (experimental − background)/(total − background). All conditions were performed in triplicate.

FACS analysis was conducted on a FACSCalibur (BD Biosciences) using Annexin V-Cy5 (BD Biosciences), anti-K^b Abs, 20.8.4s (20), and Y3 (21) for staining. For the FACS killing assay, cells were mixed at 1×10^4 targets to 5×10^4 activated effectors and incubated for 2 h. Cells were washed and then stained with Annexin V for 15 min and then washed with Annexin V calcium buffer. Kb-1BP-positive cells were gated on FL1 channel for YFP content (~100-fold higher than background autofluorescence) at levels that had comparable surface-Kb levels between treated and untreated cells and then analyzed for their percentage of Annexin V-positive in FL4 channel.

To assay stimulation of naive cells in terms of IFN-γ production, CD8$^+$ cells were mixed at 1×10^5 with an equal amount of stimulator cells in triplicate in 200 μl of medium for 48 h. Cells were centrifuged and 50 μl of supernatant was assayed for IFN-γ by ELISA. Experiments were conducted in triplicate, and ELISA was performed using an ELISA kit (catalog no. 551866; BD Biosciences) following the protocol provided, and using a Molecular Devices plate reader to acquire colorimetric measurements.

Results

Cholesterol depletion enhances class I MHC clustering

Previously we showed that cholesterol depletion reduces lateral mobility of class I MHC (10). As predicted by our model for membrane clustering (11), this change in mobility altered class I MHC clustering. Cells acutely depleted of cholesterol had larger and brighter clusters of HLA-A2 than control cells. This effect can be seen qualitatively by comparing Fig. 1, *A* and *B*, and is quantified in Fig. 1, *C* and *D*. Clusters of class I MHC molecules at or near the surface of cholesterol-depleted JY cells (Fig. 1*B*) were on average five times as bright as the clusters of class I MHC molecules at the surface of control cells (Fig. 1*A*). The average apparent size of class I MHC clusters increased slightly in cholesterol-depleted cells, from 330 ± 90 nm to 353 ± 76 nm. Although the modal value for the two populations was the same in the range 300–350 nm, there was an excess of larger clusters on the surfaces of cholesterol depleted cells. These increases in clustering were a result of redistribution of class I MHC molecules, as the total intensity of HLA-A2-YFP on the cell surface was not changed.

Cholesterol depletion enhances Ag presentation

Increased clustering due to cholesterol depletion enhanced Ag presentation in two different assays of T cell function. Cholesterol-depleted cells provoked a greater release of serine esterase from effector T cells than did control cells (Fig. 2*A*). The fraction of granzyme released by CTL stimulated by chronically LDL-deprived cells or by cells treated acutely with cholesterol oxidase was as large as that in a positive control of T cells stimulated with phorbol ester and more than 2-fold that of T cells responding to control JY cells. Consistent with their enhanced serine esterase release, CTLs killed allo-target cells depleted of cholesterol more efficiently than they killed control target cells. The results of one assay, over a range of E:T ratios are shown in Fig. 2*B*; the lysis of cholesterol-depleted cells was about twice that of control cells at a given E:T. Cholesterol depletion did not change the amount of

[5] Abbreviations used in this paper: TIRFM, total internal reflection fluorescence microscopy; CytD, cytochalasin D; YFP, yellow fluorescent protein; LDL, low-density lipoprotein.

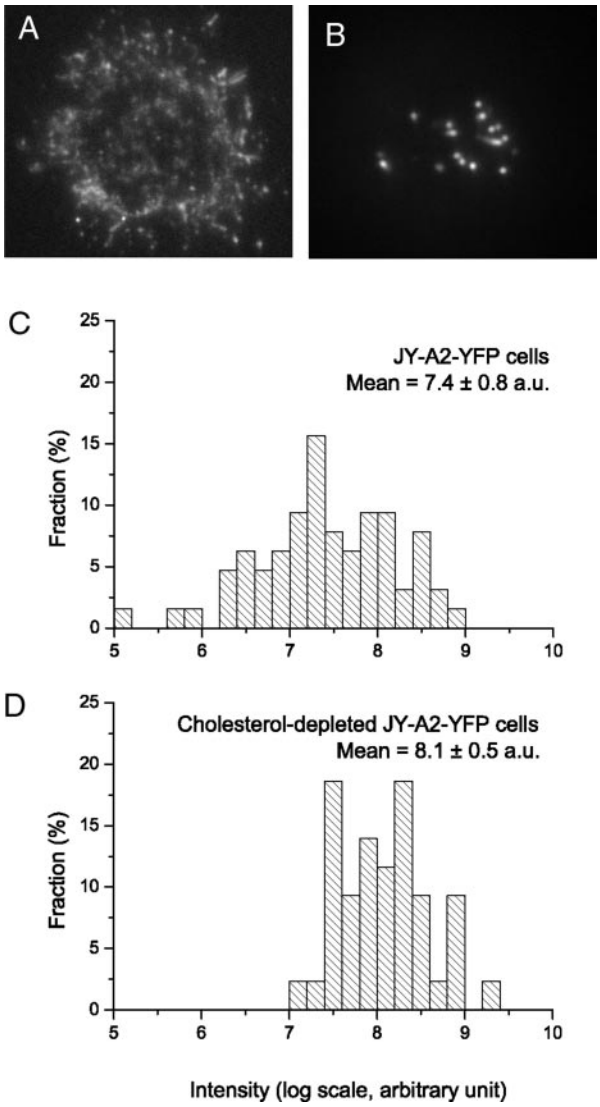

FIGURE 1. Class I clusters are larger and brighter on cholesterol-depleted cells than on control cells. JY cells were stably transfected with human class I MHC allele, HLA-A2, tagged with YFP (18). Cells were acutely depleted of cholesterol with methyl-β-cyclodextrin. TIRFM was used to image the plasma membrane of control (*A*) and cholesterol-depleted cells (*B*). Images were analyzed to determine cluster size and intensity values in arbitrary units (a.u.). Histograms of intensity (log-scale) are plotted for control cells (*C*) and cholesterol-depleted cells (*D*). The increase in cluster intensity after cholesterol depletion was statistically significant ($p < 0.001$) and the change in cluster size was statistically significant ($p < 0.05$) both by Student's *t* test.

class I molecules on the cell surface and did not change the rate of E:T conjugation, measured by flow cytometry (data not shown). Enhanced lysis after cholesterol depletion was not due to changes in the osmotic fragility of the target cells, as cholesterol-depleted and control cells were equally sensitive to lysis in hypotonic saline (data not shown).

Restoring class I mobility of cholesterol-depleted cells also restored normal Ag presentation. Our previous results (10) showed that changes in MHC mobility due to cholesterol depletion were mediated through stiffening of the actin cytoskeleton. Consistent with this finding, disrupting actin filaments restored normal MHC mobility. If enhanced presentation by class I after cholesterol depletion is due to confinement and clustering by actin filaments, we would expect that disrupting actin would reverse the effect of

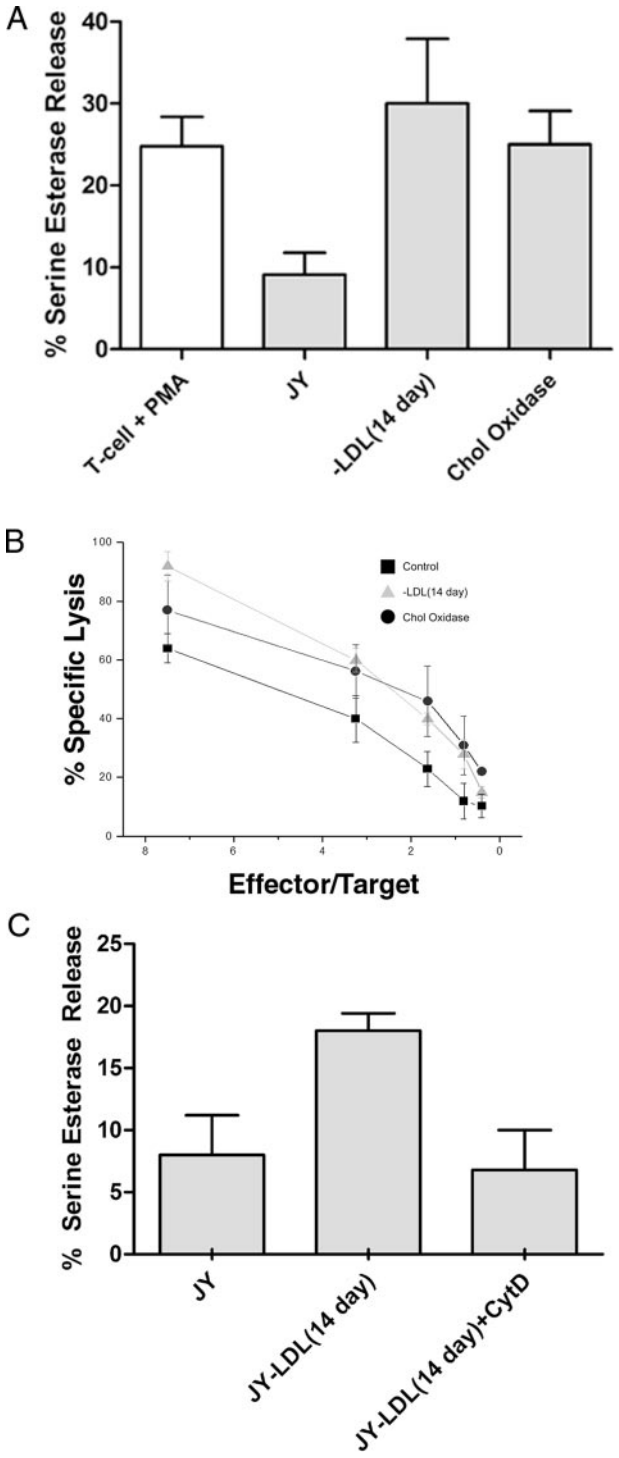

FIGURE 2. Enhanced recognition of cholesterol-depleted allogenic targets by effector CTL. Control, JY, and cells depleted of cholesterol either acutely, by cholesterol oxidase, or chronically, by growth for 14 days in LDL-deficient medium, were used as targets for alloreactive T effectors. *A*, Cholesterol-depleted cells provoked higher serine esterase release from effector cells as compared with control cells. Maximal release was induced by treatment of the T cells plus 40 ng/ml PMA (T+PMA). *B*, Enhanced T cell recognition was also manifested as enhanced lysis of ^{51}Cr-labeled JY target cells after cholesterol depletion. At all E:T ratios, cholesterol-depleted cells were lysed to a greater extent than were control cells. *C*, Disrupting actin filaments reversed the effects of cholesterol depletion. Pretreating cholesterol-depleted target cells with 5 μg/ml CytD for 30 min reduced serine esterase release by T effectors. The error bars represent SD.

cholesterol depletion. This expectation was the case. When cholesterol-depleted cells were treated with an actin depolymerizer, CytD, for 30 min before incubation with effector cells, T effector response, as measured by serine esterase release, was reduced to control levels (Fig. 2*C*). Control cells treated with CytD alone were as effective at stimulating serine esterase release as untreated cells. Similar effect was seen in CTL-mediated killing by assayed chromium release; cholesterol-depleted targets produced lower ^{51}Cr release when pretreated with CytD, whose effect is only slowly reversible, than without treatment (data not shown).

Enhancing clustering enhances recognition of scarce agonist peptides

The peptides recognized by alloreactive CTL are poorly defined. To better understand the mechanism of enhanced recognition after cholesterol depletion, we investigated peptide-specific recognition and lysis using CTLs from the 2C transgenic mouse. The 2C TCR recognizes the SIY peptide in the context of the mouse class I MHC molecules H2-K^b as a strong agonist, recognizes the p2CA peptide as a weak agonist, and does not respond to the SIN peptide (1). We used a TAP-deficient cell line, T2, expressing H2-K^b, to load H2-K^b specifically, with peptide of our choice at different levels. This allowed us to measure effects of cholesterol depletion for a range of peptides and over a wide range of surface concentrations of peptide-MHC. When target cells were loaded at high agonist peptide (SIY) concentrations (10 μM), cholesterol depletion modestly enhanced (10%) cell lysis at a range of E:T ratios. However, when cells were loaded at 1000-fold lower concentrations of agonist peptide (10 nM), cholesterol depletion enhanced cell lysis by ~50% (Fig. 3*A*).

The enhancements due to cholesterol depletion as a function of peptide concentration are summarized in Fig. 3, *B–D*. Optimal enhancements were seen in the 1–100 nM range SIY peptide (Fig. 3*B*). Cholesterol depletion had an even larger effect on the killing of cells loaded with the weak agonist peptide, p2CA, whose affinity for the H2-K^b and 2C TCR is 1000-fold lower than SIY (1). At low concentrations of p2CA, killing was enhanced by over 80% (Fig. 3*C*). At higher concentrations of p2CA, cholesterol depletion did not enhance and actually showed a decrease in killing. Nonspecific killing of null peptide, SIN, loaded cells was not enhanced by cholesterol depletion at any concentration; indeed, there was some reduction in basal lysis (Fig. 3*D*). If peptide levels were titrated sufficiently low, or no peptide was added at all (Fig. 3*C*), cholesterol depletion reduced presentation. Overall, cholesterol depletion greatly enhanced presentation at low peptide concentrations of agonist peptide. At other concentrations, effects of cholesterol depletion varied from smaller enhancements to inhibition of presentation.

Clustering class I MHC molecules by direct cross-linking enhances recognition of scarce agonist peptides

Although cholesterol depletion can be used to cluster MHC, it may have other consequences for the cell (22). Given the correlation between enhanced clustering and enhanced killing, we tested whether aggregating class I MHC independently of cholesterol depletion would enhance recognition by CTLs. We engineered an H2-K^b tagged with a YFP and a single binding domain for an analog of FK506. This construct, Kb-1BP, dimerizes in cells upon the addition of a membrane-permeable, divalent analog of FK506, AP20187 (23). We reasoned that dimerizing class I molecules would stabilize and enhance pre-existing class I MHC clusters (Fig. 4*A*). Confocal images of the upper surface of cells expressing our cross-linkable construct, Kb-1BP showed an increase in cluster size and intensity (Fig. 4, *B–E*) after adding dimerizer. Consistent

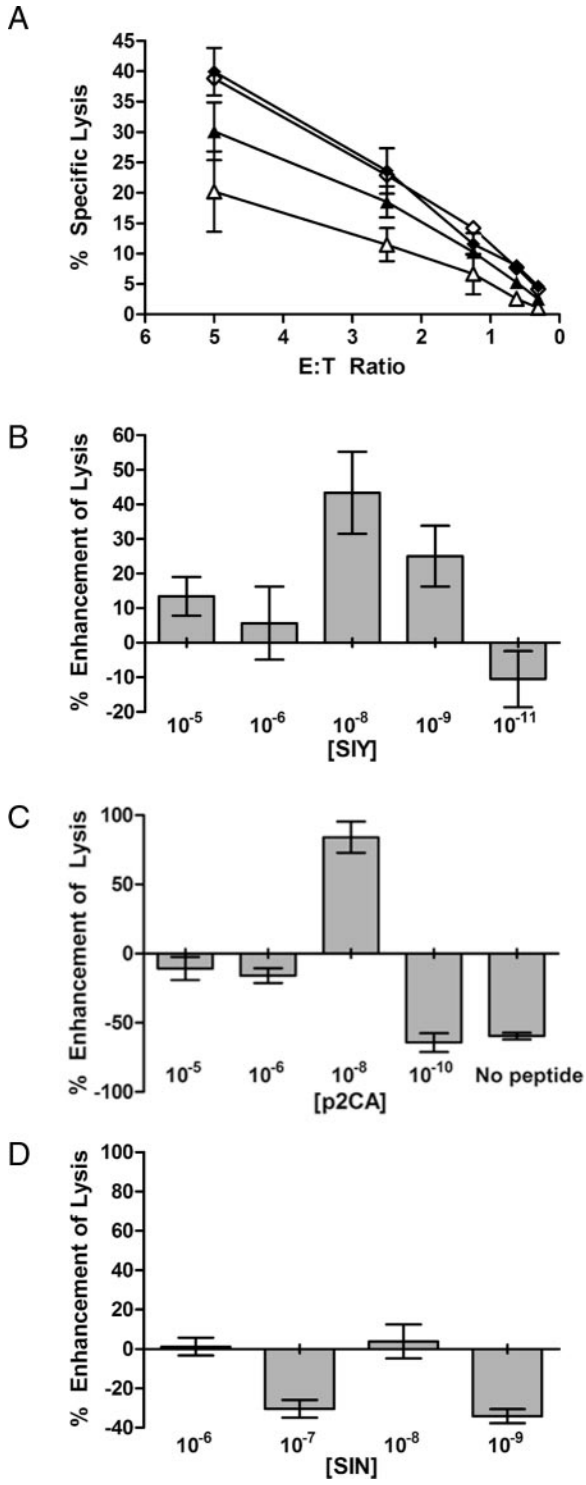

FIGURE 3. Peptide-specific T cell responses are enhanced by cholesterol depletion of targets. T2-Kb target cells were chronically depleted of cholesterol for 3–7 days before loading with peptide. *A*, Cells were loaded with 10 μM (◇) or 10 nM (△) of strong agonist peptide, SIY, and depleted of cholesterol (filled) or untreated (open); specific lysis is shown as a function of E:T ratio. Cholesterol depletion had no effect at high peptide levels, but at lower levels, depletion enhanced lysis at all E:T ratios. *B–D*, Changes in lysis due to cholesterol depletion are shown over a range of peptide concentrations. Peptide concentrations are given as molarity. *C*, Cholesterol depletion of empty peptide reduced nonspecific lysis. Depending on peptide concentration and E:T ratio, specific lysis would vary from 5 to 50% between experiments. To normalize percentage changes, comparisons between treated and controls were analyzed at E:T ratios in which the control lysis was between 10 and 30%. The error bars represent SE.

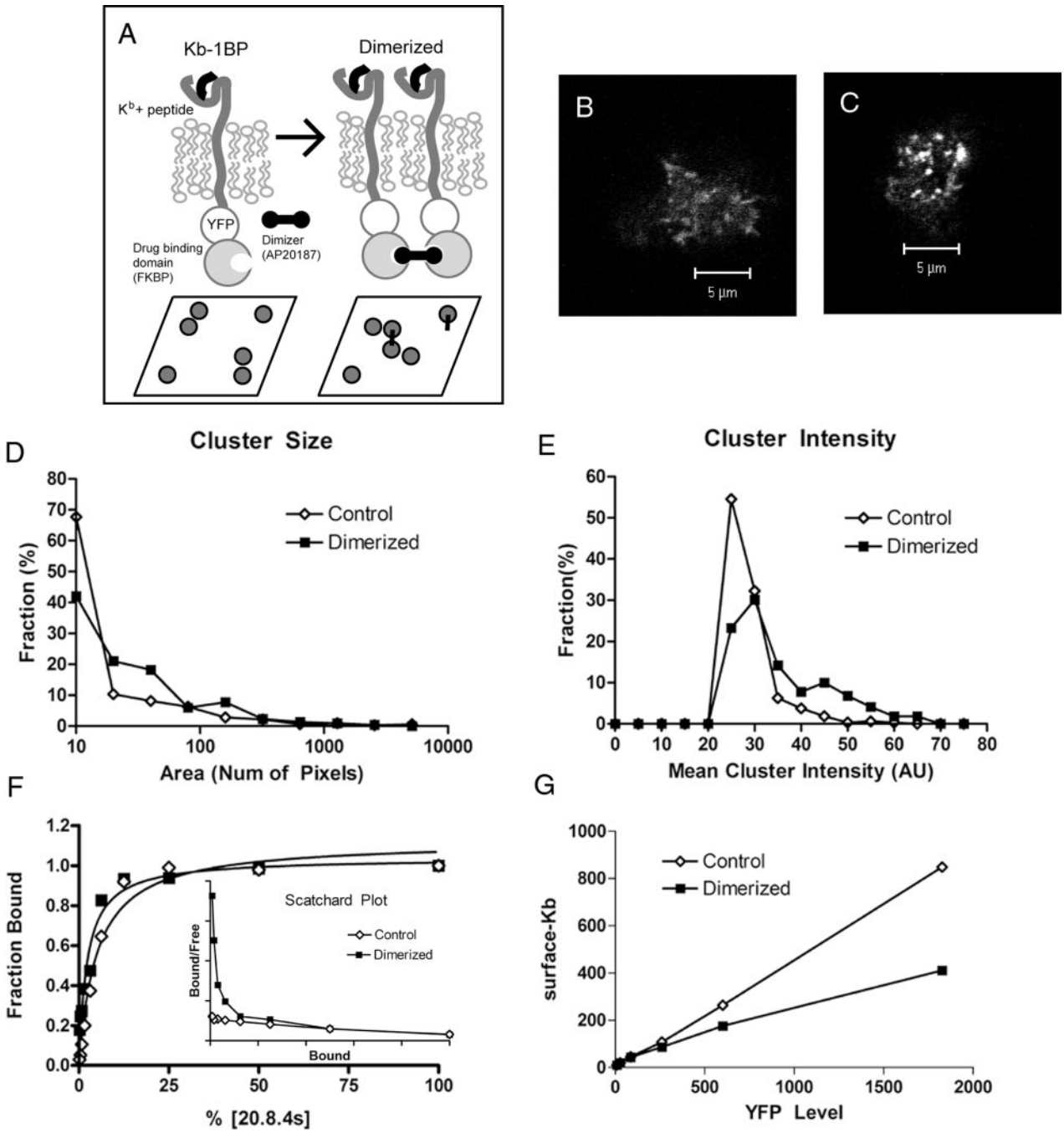

FIGURE 4. Dimerizing K^b and clustering class I MHC. *A*, A YFP-tagged, cross-linkable H2-K^b construct, and a model for how dimerization may induce larger clusters on the cell surface. *B* and *C*, T2 cells expressing Kb-1BP were imaged by confocal microscopy at the cell surface distal to the coverslip. Dimerization increased the frequency of brighter and larger clusters. Sample images of control cells (*B*) and cells treated with dimerizer (*C*) are shown. Histograms of cluster size (*D*) and mean intensity (*E*) show that these changes were statistically significant ($p < 0.0001$ and $p < 0.05$, respectively) for $n = 16$ cells with 500+ clusters. *F*, Titrating binding using 20.8.4s against an epitope in α_1/α_2 showed a significantly higher affinity for cells treated with dimerizer (filled) than compared with untreated cells. Three independent data sets were normalized and then fit by nonlinear least squares to a one-site binding model. The apparent K_d for mAb changed from 5.1 to 2.3 arbitrary units (AU) upon dimerization indicating higher affinity, and this change was significant ($p < 0.05$). *F*, The Scatchard plot (*inset*) for the two binding curves shows dimerization of Kb-1BP creates high-affinity binding sites for 20.8.4s. Dimerization also resulted in induced endocytosis of Kb-1BP construct. *G*, Ab staining of surface H2-K^b is plotted as function of YFP, indicating levels of expressed Kb-1BP in T2 cells. Dimer-treated cells (filled) showed reduced surface Kb levels compared with untreated cells (open) at any particular YFP level.

with this result, the avidity of Ab binding to α_1/α_2 domain of H2-K^b (24) increased after dimerization (Fig. 4*F*). The avidity of a second Ab, Y3, whose binding has only partially been mapped (21), and has a much lower affinity for H2-K^b was unchanged. There was also an unexpected 2-fold reduction in overall surface H2-K^b levels (Fig. 4*G*) upon the addition of dimerizer; this probably reflects induced endocytosis of MHC clusters (25).

We measured 2C CTL-mediated killing of target cells transiently expressing Kb-1BP with or without the dimerizer. These cells showed a wide distribution of Kb-1BP surface expression

levels, depending on efficiency of transfection and dimerizer concentration. Cells treated with 10 nM dimerizer for 2 h had half the surface Kb-1BP of untreated cells for any particular YFP expression level. However, to investigate the effects of clustering on lysis of target cells, we needed to compare treated and untreated expressing equal levels of surface H2-Kb. Therefore we used FACS to gate cell populations in terms of YFP fluorescence that would correspond to comparable levels of surface K^b as shown in Fig. 4*G*. We measured apoptosis by staining with Annexin V and compared the difference in Annexin V-positive cells after dimerization (Fig. 5*A*). Upon clustering of Kb-1BP, there was an enhancement of T cell mediated apoptosis by 60–90% at low SIY agonist peptide concentrations (Fig. 5*B*). At high concentrations of agonist, we saw no increase in presentation due to clustering. Again, inducing class I dimerization on cells loaded with the weak agonist, p2CA, increased cell killing at low concentrations and decreased it at high concentrations (Fig. 5*C*), consistent with the data from cholesterol depletion. The dimerizer did not enhance killing of T2-K^b lacking the 1-bp domain (data not shown).

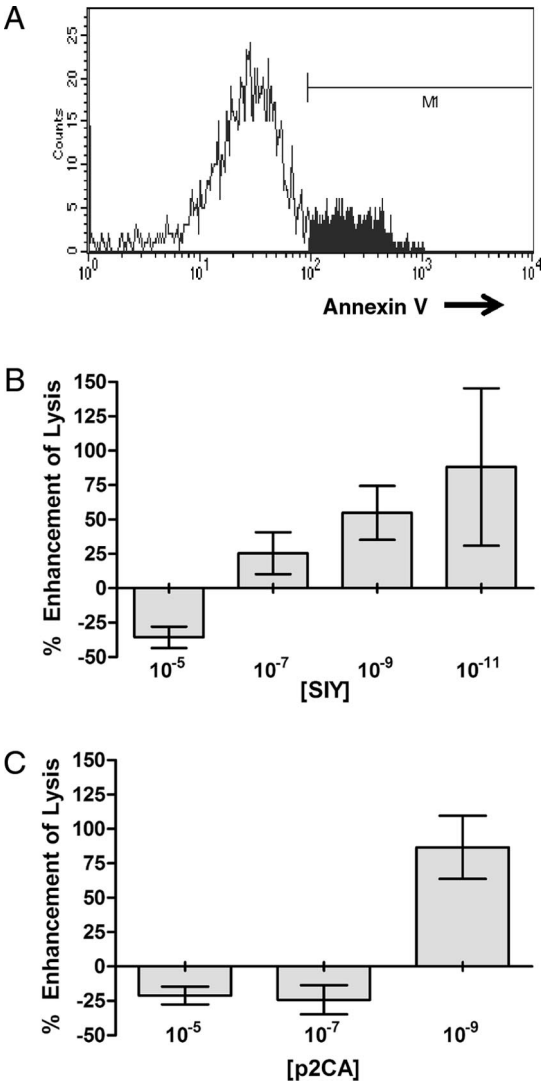

FIGURE 5. Enhanced recognition of scarce peptide after clustering of Kb-1BP. T2 cells were transiently transfected with Kb-1BP. Cells were peptide pulsed, as before, treated or not with dimerizing drug, and incubated with 2C effector T cells. *A*, Killing was measured in terms of staining with Annexin V-Cy5, detecting apoptotic cells for populations that gated for comparable levels of surface H2-K^b as assessed by flow cytometry (as shown in Fig. 4*G*). *B* and *C*, The percentage increase in Annexin V-positive cells after dimerization of H2-K^b is plotted as a function of SIY and p2CA peptide concentration. The error bars represent SE.

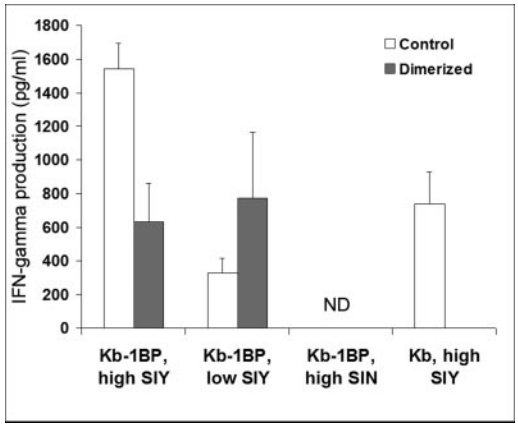

FIGURE 6. Enhanced stimulation of naive T cells by APCs with clustered scarce peptide activation of naive $CD8^+$ 2C T cells stimulated by T2 cells expressing Kb-1BP is enhanced by clustering. Cells were loaded with agonist or null peptide and either untreated (□) or treated with dimerizer (▨). Effectors and stimulators were incubated for 2 days, and supernatants were assayed for IFN-γ production by ELISA. The error bars represent SE. ND, not detectable.

The effect of clustering MHC on enhanced recognition by T cells was not limited to effector cells. We measured activation of naive $CD8^+$ 2C T cells in terms of IFN-γ production stimulated by Kb-1BP under various conditions. Dimerizing the stimulating Ag enhanced agonist recognition after loading with low nanomolar concentrations of peptide, while it reduced recognition after loading with high micromolar concentrations of peptide (Fig. 6).

Discussion

Class I MHCs are clustered on the cell surface. To assess the functional consequences of clustering, we developed two methods to enhance the size of MHC clusters, cholesterol depletion and specific cross-linking of an engineered MHC molecule. Overall, clustering by cholesterol depletion and dimerization produced similar effects in presentation. However, at certain concentrations of peptide, the effective changes differed between treatments. These discrepancies may be due to a difference in the size and nature of clusters generated by the two treatments. They may also be due to technical reasons; we required different assays for the effects of the two treatments, therefore the data in Figs. 3 and 5 may not be equivalent. Nevertheless, clustering by either method enhanced recognition of peptide-MHC by T cells, especially when agonist peptide was scarce.

Both acute and chronic depletion of target cell cholesterol enhanced granzyme, serine esterase, release by activated effector CTL. Enhanced T cell responses also translated into enhanced lysis of target cells. Alloreactive T cells killed APCs with clustered MHC more efficiently than they killed control target cells. These effects were seen at all E:T ratios. Conversely, dispersion of clusters on cholesterol-depleted cells returned their presentation to control levels. As we mentioned earlier, we argue that the effects on class I mobility and clustering by cholesterol depletion are mediated through the actin cytoskeleton (10). Stiffening and loosening the actin cytoskeleton using various actin filament drugs produced the same effects on presentation as predicted.

When we switched to a peptide-specific model of recognition, we could only enhance killing at low concentration of agonist peptide. This result is consistent with the idea that allorecognition

involves only a subset of the peptides represented on the surface and that clustering may facilitate T cell scanning for cognate peptide. If lysis was enhanced at all concentrations of agonist, one could argue that the functional consequences of cholesterol depletion were downstream of agonist recognition. Moreover, if lysis was also enhanced in the case of nonspecific peptide or no added peptide, one could argue that recognition by T cells did not play a role in the effects seen. However, we only saw enhancement at low agonist peptide concentrations, which argues strongly that the changes we found were due to changes in the efficiency of presentation.

Clustering class I MHC by cross-linking engineered H2-K^b molecules confirmed and extended our functional results on clustering of class I MHC molecules by cholesterol depletion. Microscopy shows that dimerizing MHC molecules stabilizes and amalgamates the small clusters of MHC present on APC surfaces.

Different peptides produced different effects when clustered. In the case of cells presenting high concentrations of SIY agonist, we saw weak enhancement of lysis after cholesterol depletion and saw some reduction after dimerizing Kb-1BP. We argue that at high levels of strong agonist, T cells are efficiently activated; therefore, clustering has a small effect on recognition. As we titrated down the levels of agonist peptide, recognition was less efficient, and clustering enhanced it. This was seen even more clearly when cells were loaded with the weak agonist peptide, p2CA, whose recognition by T cells is inefficient. Clustering class I MHC on cells loaded with low concentrations of p2CA enhanced specific lysis to almost double that of controls while at high concentrations of p2CA, clustering actually inhibited recognition. In most cases, enhancement seemed to peak at nanomolar concentrations and would in some cases drop off at very low concentrations.

Clusters may enhance recognition by providing multiple local copies of some peptide-MHC or by enhancing T cell residence time on a target cell. Normally, scarce agonist peptides are presented in a sea of self-peptide. Clustering of class I MHC molecules would cause a reduction in their rotational and lateral diffusion as compared with monomers on the plasma membrane. These large, slowly rotating lattices of class I MHC could enhance recognition by providing T cells with stable local densities of class I MHC plus peptide combinations to sample. Because TCR can dock on a class I MHC in a variety of orientations and tilts (26), cluster of class I may also facilitate proper docking and reduce scan time for TCR sampling. In addition, as some TCRs may exist as clusters as well, engaging clusters from both the T cell and APC side may provide efficient activation.

Clusters of MHC may also function to provide simultaneous sampling of self- and non-self peptide by multiple TCR in a membrane domain. At high concentrations of strong agonist, the density of signal is more than sufficient and clustering may not be necessary for recognition, as was seen in our results with SIY peptide. However, in the absence of strong agonist at high surface concentrations, the sampling of bouquets of self and agonist may be a way T cells can differentiate minute class I MHC peptide differences to make dramatically different outcomes for activation. It is important to note that in our peptide-loading model, APCs were loaded in the presence of serum. At high concentrations of peptide with high affinity for MHC, such as SIY or SIN, serum proteins probably had little effect on surface loading of MHC. However at low concentrations of agonist, serum was likely to contribute nonspecific, nonactivating peptides to the surface display. In the case of weak agonist, p2CA, with weak affinities and short k_{off} for the TCR (1), the role of nonspecific peptide may be particularly important for recognition. This may explain why at low concentrations, clustering had such a strong effect on p2CA recognition. It may also explain the negative effects clustering had on presentation of high concentrations of p2CA. Clustering high concentrations of weak agonist might produce a "bland" signal, and may read too similar to a null peptide when presented in the absence of null peptide. This also suggests that the choice of null peptide would play an important role in effective detection of weak agonists as others have suggested for class II MHC (27).

From our results, we would not be surprised to find that professional APCs modulate class I clustering to modulate Ag presentation. Others have shown IFN-γ treatment, known to up-regulate class I levels, also reorganizes class I on the cell surface (28, 29). This change could enhance presentation to and activation of naive T cells. In contrast, it may be that dispersion of clusters or their absence on some APCs (6) leads to T cell anergy rather than activation. It is unclear to what degree cells regulate class I clusters in terms of size and stability, but from their functional importance in presentation, clusters may likely be regulated in an inducible manner.

Taken together, these data suggest that MHC organization plays an important role in modulating T cell sensitivity for agonist peptide. Clustering MHC may enhance recognition of weak or rare epitopes in cancer and viral vaccine models. One direction others have taken in cancer immunology has been to identify and expand the number of oncogenic epitopes recognized by ex vivo-stimulated tumor infiltrating lymphocytes (30). Clustering class I on these ex vivo stimulations may expand the repertoire of T cell clones stimulated thereby enhancing the engendered response.

Acknowledgments

We thank Jonathan Schneck, Kapil Gupta, and Joan Bieler (Department of Pathology, JHMI) for maintaining and providing 2C cells and many helpful discussions. We thank Antony Rosen (Department of Rheumatology, JHMI) for help with the granzyme release assay.

Disclosures

The authors have no financial conflict of interest.

References

1. Sykulev, Y., Y. Vugmeyster, A. Brunmark, H. L. Ploegh, and H. N. Eisen. 1998. Peptide antagonism and T cell receptor interactions with peptide-MHC complexes. *Immunity* 9: 475–483.
2. Sykulev, Y., M. Joo, I. Vturina, T. J. Tsomides, and H. N. Eisen. 1996. Evidence that a single peptide-MHC complex on a target cell can elicit a cytolytic T cell response. *Immunity* 4: 565–571.
3. Wülfing, C., C. Sumen, M. D. Sjaastad, L. C. Wu, M. L. Dustin, and M. M. Davis. 2002. Costimulation and endogenous MHC ligands contribute to T cell recognition. *Nat. Immunol.* 3: 42–47.
4. Purbhoo, M. A., D. J. Irvine, J. B. Huppa, and M. M. Davis. 2004. T cell killing does not require the formation of a stable mature immunological synapse. *Nat. Immunol.* 5: 524–530.
5. Yachi, P. P., J. Ampudia, N. R. Gascoigne, and T. Zal. 2005. Nonstimulatory peptides contribute to antigen-induced CD8-T cell receptor interaction at the immunological synapse. *Nat. Immunol.* 6: 785–792.
6. Matko, J., Y. Bushkin, T. Wei, and M. Edidin. 1994. Clustering of class I HLA molecules on the surfaces of activated and transformed human cells. *J. Immunol.* 152: 3353–3360.
7. Vereb, G., J. Matko, G. Vamosi, S. M. Ibrahim, E. Magyar, S. Varga, J. Szollosi, A. Jenei, R. Gaspar, Jr., T. A. Waldmann, and S. Damjanovich. 2000. Cholesterol-dependent clustering of IL-2Rα and its colocalization with HLA and CD48 on T lymphoma cells suggest their functional association with lipid rafts. *Proc. Natl. Acad. Sci. USA* 97: 6013–6018.
8. Bodnár, A., Z. Bacsó, A. Jenei, T. M. Jovin, M. Edidin, S. Damjanovich, and J. Matkó. 2003. Class I HLA oligomerization at the surface of B cells is controlled by exogenous β_2-microglobulin: implications in activation of cytotoxic T lymphocytes. *Int. Immunol.* 15: 331–339.
9. Bodnár, A., A. Jenei, L. Bene, S. Damjanovich, and J. Matko. 1996. Modification of membrane cholesterol level affects expression and clustering of class I HLA molecules at the surface of JY human lymphoblasts. *Immunol. Lett.* 54: 221–226.
10. Kwik, J., S. Boyle, D. Fooksman, L. Margolis, M. P. Sheetz, and M. Edidin. 2003. Membrane cholesterol, lateral mobility, and the phosphatidylinositol 4,5-bisphosphate-dependent organization of cell actin. *Proc. Natl. Acad. Sci. USA* 100: 13964–13969.
11. Gheber, L. A., and M. Edidin. 1999. A model for membrane patchiness: lateral diffusion in the presence of barriers and vesicle traffic. *Biophys. J.* 77: 3163–3175.

12. Ritchie, K., R. Iino, T. Fujiwara, K. Murase, and A. Kusumi. 2003. The fence and picket structure of the plasma membrane of live cells as revealed by single molecule techniques (review). *Mol. Membr. Biol.* 20: 13–18.
13. Salter, R. D., and P. Cresswell. 1986. Impaired assembly and transport of HLA-A and -B antigens in a mutant TxB cell hybrid. *EMBO J.* 5: 943–949.
14. Chen, W., F. R. Carbone, and J. McCluskey. 1993. Electroporation and commercial liposomes efficiently deliver soluble protein into the MHC class I presentation pathway: priming in vitro and in vivo for class I-restricted recognition of soluble antigen. *J. Immunol. Methods* 160: 49–57.
15. Sykulev, Y., A. Brunmark, T. J. Tsomides, S. Kageyama, M. Jackson, P. A. Peterson, and H. N. Eisen. 1994. High-affinity reactions between antigen-specific T-cell receptors and peptides associated with allogeneic and syngeneic major histocompatibility complex class I proteins. *Proc. Natl. Acad. Sci. USA* 91: 11487–11491.
16. Spiliotis, E. T., T. Pentcheva, and M. Edidin. 2002. Probing for membrane domains in the endoplasmic reticulum: retention and degradation of unassembled MHC class I molecules. *Mol. Biol. Cell* 13: 1566–1581.
17. Zacharias, D. A., J. D. Violin, A. C. Newton, and R. Y. Tsien. 2002. Partitioning of lipid-modified monomeric GFPs into membrane microdomains of live cells. *Science* 296: 913–916.
18. Pentcheva, T., and M. Edidin. 2001. Clustering of peptide-loaded MHC class I molecules for endoplasmic reticulum export imaged by fluorescence resonance energy transfer. *J. Immunol.* 166: 6625–6632.
19. Taffs, R., and M. V. Sitkovsky. 1998. Granzyme enzyme exocytosis assay for cytotoxic T lymphocyte activation. In *Current Protocols In Immunology*. John Wiley & Sons, p. 3.16.1–3.16.3.
20. Ozato, K., and D. H. Sachs. 1981. Monoclonal antibodies to mouse MHC antigens. III. Hybridoma antibodies reacting to antigens of the H-2^b haplotype reveal genetic control of isotype expression. *J. Immunol.* 126: 317–321.
21. Hämmerling, G. J., E. Rusch, N. Tada, S. Kimura, and U. Hämmerling. 1982. Localization of allodeterminants on H-$2K^b$ antigens determined with monoclonal antibodies and H-2 mutant mice. *Proc. Natl. Acad. Sci. USA* 79: 4737–4741.
22. Unruh, T. L., H. Li, C. M. Mutch, N. Shariat, L. Grigoriou, R. Sanyal, C. B. Brown, and J. P. Deans. 2005. Cholesterol depletion inhibits src family kinase-dependent calcium mobilization and apoptosis induced by rituximab crosslinking. *Immunology* 116: 223–232.
23. Clackson, T., W. Yang, L. W. Rozamus, M. Hatada, J. F. Amara, C. T. Rollins, L. F. Stevenson, S. R. Magari, S. A. Wood, N. L. Courage, et al. 1998. Redesigning an FKBP-ligand interface to generate chemical dimerizers with novel specificity. *Proc. Natl. Acad. Sci. USA* 95: 10437–10442.
24. Stroynowski, I., J. Forman, R. S. Goodenow, S. G. Schiffer, M. McMillan, S. O. Sharrow, D. H. Sachs, and L. Hood. 1985. Expression and T cell recognition of hybrid antigens with amino-terminal domains encoded by Qa-2 region of major histocompatibility complex and carboxyl termini of transplantation antigens. *J. Exp. Med.* 161: 935–952.
25. Makkerh, J. P., C. Ceni, D. S. Auld, F. Vaillancourt, G. Dorval, and P. A. Barker. 2005. p75 neurotrophin receptor reduces ligand-induced Trk receptor ubiquitination and delays Trk receptor internalization and degradation. *EMBO Rep.* 6: 936–941.
26. Grasberger, B., A. P. Minton, C. DeLisi, and H. Metzger. 1986. Interaction between proteins localized in membranes. *Proc. Natl. Acad. Sci. USA* 83: 6258–6262.
27. Krogsgaard, M., Q. J. Li, C. Sumen, J. B. Huppa, M. Huse, and M. M. Davis. 2005. Agonist/endogenous peptide-MHC heterodimers drive T cell activation and sensitivity. *Nature* 434: 238–243.
28. Bacsó, Z., L. Bene, L. Damjanovich, and S. Damjanovich. 2002. IFN-γ rearranges membrane topography of MHC-I and ICAM-1 in colon carcinoma cells. *Biochem. Biophys. Res. Commun.* 290: 635–640.
29. Bene, L., A. Bodnár, S. Damjanovich, G. Vámosi, Z. Bacsó, J. Aradi, A. Berta, and J. Damjanovich. 2004. Membrane topography of HLA I, HLA II, and ICAM-1 is affected by IFN-γ in lipid rafts of uveal melanomas. *Biochem. Biophys. Res. Commun.* 322: 678–683.
30. Dudley, M. E., J. R. Wunderlich, T. E. Shelton, J. Even, and S. A. Rosenberg. 2003. Generation of tumor-infiltrating lymphocyte cultures for use in adoptive transfer therapy for melanoma patients. *J. Immunother.* 26: 332–342.